Chapter 8

Maximum Power Extraction from Utility-Interfaced Wind Turbines

Ali M. Eltamaly, A. I. Alolah and Hassan M. Farh

Additional information is available at the end of the chapter

http://dx.doi.org/10.5772/54675

1. Introduction

Wind energy is one of the most promising renewable energy resources for producing electricity due to its cost competitiveness compared to other conventional types of energy resources. It takes a particular place to be the most suitable renewable energy resources for electricity production. It isn't harmful to the environment and it is an abundant resource available in nature. Hence, wind power could be utilized by mechanically converting it to electrical power using wind turbine, WT. Various WT concepts have a quick development of wind power technologies and significant growth of wind power capacity during last two decades. Variable speed operation and direct drive WTs have been the modern developments in the technology of wind energy conversion system, WECS. Variable-speed operation has many advantages over fixed-speed generation such as increased energy capture, operation at MPPT over a wide range of wind speeds, high power quality, reduced mechanical stresses, aerodynamic noise improved system reliability, and it can provide (10-15) % higher output power and has less mechanical stresses in comparison with the operation at a fixed speed [1, 2]. WTs can be classified according to the type of drive train into direct drive (DD) and gear drive (GD). The GD type uses a gear box, squirrel cage induction generator (SCIG) and classified as stall, active stall and pitch control WT and work in constant speed applications. The variable speed WT uses doubly-fed induction generator, (DFIG) especially in high power WTs. The gearless DD WTs have been used with small and medium size WTs employing permanent-magnet synchronous generator (PMSG) with higher numbers of poles to eliminate the need for gearbox which can be translated to higher efficiency. PMSG appears more and more attractive, because the advantages of permanent magnet, (PM) machines over electrically excited machines such as its higher efficiency, higher energy yield, no additional power supply for the magnet field excitation and higher reliability due to the absence of mechanical components such as slip

rings. In addition, the performance of PM materials is improving, and the cost is decreasing in recent years. Therefore, these advantages make direct-drive PM wind turbine systems more attractive in application of small and medium-scale wind turbines [1, 3-4].

Robust controller has been developed in many literatures [5-15] to track the maximum power available in the wind. They include tip speed ratio (TSR) [5, 13], power signal feedback (PSF) [8, 14], and the hill-climb searching (HCS) [11-12] methods. The TSR control method regulates the rotational speed of the generator to maintain an optimal TSR at which power extracted is maximum [13]. For TSR calculation, both the wind speed and turbine speed need to be measured, and the optimal TSR must be given to the controller. The first barrier to implement TSR control is the wind speed measurement, which adds to system cost and presents difficulties in practical implementations. The second barrier is the need to obtain the optimal value of TSR, this value is different from one system to another. This depends on the turbine-generator characteristics results in custom-designed control software tailored for individual wind turbines [14]. In PSF control [8, 14], it is required to have the knowledge of the wind turbine's maximum power curve, and track this curve through its control mechanisms. The power curves need to be obtained via simulations or off-line experiment on individual wind turbines or from the datasheet of WT which makes it difficult to implement with accuracy in practical applications [7-8, 15]. The HCS technique does not require the data of wind, generator speeds and the turbine characteristics. But, this method works well only for very small wind turbine inertia. For large inertia wind turbines, the system output power is interlaced with the turbine mechanical power and rate of change in the mechanically stored energy, which often renders the HCS method ineffective [11-12]. On the other hand, different algorithms have been used for maximum power extraction from WT in addition to the three method mentioned above. For example, Reference [1] presents an algorithm for maximum power extraction and reactive power control of an inverter through the power angle, δ of the inverter terminal voltage and the modulation index, m_a based variable-speed WT without wind speed sensor. Reference [16] presents an algorithm for MPPT via controlling the generator torque through q-axis current and hence controlling the generator speed with variation of the wind speed. These techniques are used for a decoupled control of the active and reactive power from the WT through q-axis and d-axis current respectively. Also, reference [17] presents a decoupled control of the active and reactive power from the WT, independently through q-axis and d-axis current but maximum power point operation of turbine system has been produced through regulating the input dc current of the dc/dc boost converter to follow the optimized current reference [17]. Reference [18] presents an algorithm for MPPT through directly adjusting duty ratio of the dc/dc boost converter and modulation index of the PWM- VSC. Reference [19] presents MPPT control algorithm based on measuring the dc-link voltage and current of the uncontrolled rectifier to attain the maximum available power from wind. Finally, references [20-22] present MPPT control based on a fuzzy logic control (FLC). The function of FLC is to track the generator speed with the reference speed for maximum power extraction at variable speeds. The MPPT algorithms can be divided into two categories, the first one is MPPT algorithms for WT with wind speed sensor and the second one is MPPT algorithms without wind speed sensor (sensorless MPPT controller). Wind speed sensor normally used in conventional wind energy conversion systems, WECS [10, 23] for implementing MPPT control algorithm. This algorithm

http://dx.doi.org/10.5772/54675

increases cost and reduces the reliability of the WECS in addition to inaccuracies in measuring the wind speed. Therefore, some MPPT control methods estimate the wind speed; however, many of them require the knowledge of air density and mechanical parameters of the WECS [88-92]. Such methods require turbine generator characteristics result in custom-design software tailored for individual wind turbines. Air density, on the other hand, depends upon climatic conditions and may vary considerably over various seasons. Therefore, this technique is not favorite in modern design of WT and a lot of research efforts are focused on developing wind speed sensorless MPPT controller which does not require the knowledge of air density and turbine mechanical parameters [1, 9-11, 22-25]. Therefore, the cost and maintenance of the power control system is decreased and implementation of the power control system is not difficult compared to the sensored MPPT controller.

2. Wind Energy Conversion Systems (WECS)

Figure 1 shows the schematic diagram of the variable-speed wind energy conversion system based on a synchronous generator. This system is directly connected to the grid through power conversion system. There are two common types of the power conversion systems, the first configuration is a back-to-back PWM-VSC connected to the grid. This configuration has a lot of switches, which cause more losses and voltage stress in addition to the presence of Electromagnetic Interference (EMI). The presence of a dc-link capacitor in PWM-VSC system provides a decoupling between the two converters, it separates the control between these two converters, allowing compensation of asymmetry of both on the generator side and on the grid side, independently [16]. The second configuration consists of a diode-bridge rectifier, a boost converter and a PWM-VSC connected to the grid. This configuration is, simple, less expensive, robust, and rigid and needs simple control system. But, with this configuration the control of the generator power factor is not possible, which in turn, affects generator efficiency. Also, high harmonic distortion currents are obtained in the generator that reduce efficiency and produce torque oscillations [22].

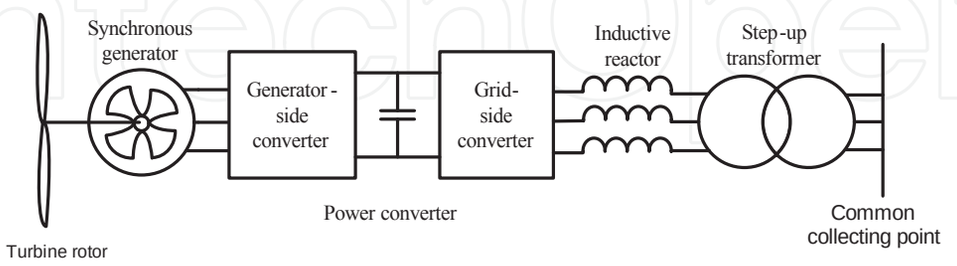

Figure 1. Wind energy conversion system based on a synchronous generator [26].

Wind turbine converts the wind power to a mechanical power, which in turn, runs a generator to generate electrical power. The mechanical power generated by wind turbine can be expressed as [15]:

$$P_m = \frac{1}{2} C_P(\lambda, \beta) \rho A u^3 \tag{1}$$

where

C_p: Turbine power coefficient.

ρ: Air density (kg/m^3).

A: Turbine sweeping area (m^2).

u: wind speed (m/s).

λ: tip speed ratio of the wind turbine which is given by the following equation [1];

$$\lambda = \frac{r_m \omega_r}{u} \tag{2}$$

Where r_m is the turbine rotor radius, ω_r is the angular velocity of turbine (rad/s).

The turbine power coefficient, C_p, describes the power extraction efficiency of the wind turbine. It is a nonlinear function of both tip speed ratio, λ and the blade pitch angle, β. While its maximum theoretical value is approximately 0.59, it is practically between 0.4 and 0.45 [15]. There are many different versions of fitted equations for C_p made in the literatures. A generic equation has been used to model $C_p(\lambda, \beta)$ and based on the modeling turbine characteristics as shown in the following equation [27]:

$$C_P(\lambda, \beta) = 0.5176\left(116 * \frac{1}{\lambda_i} - 0.4\beta - 5\right) e^{-\frac{21}{\lambda_i}} + 0.0068\lambda \tag{3}$$

With

$$\frac{1}{\lambda_i} = \frac{1}{\lambda + 0.08\beta} - \frac{0.035}{1 + \beta^3} \tag{4}$$

The C_p-λ characteristics, for different values of the pitch angle β, are illustrated in Figure 2. The maximum value of C_p is achieved for $\beta = 0$ degree and for λ_{opt}. The particular value of λ is defined as the optimal value (λ_{opt}). Continuous operation of wind turbine at this point guarantees the maximum available power which can be harvested from the available wind at any speed.

http://dx.doi.org/10.5772/54675

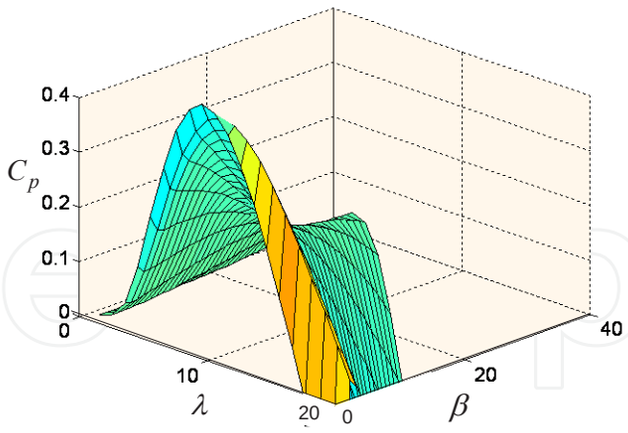

Figure 2. Aerodynamic power coefficient variation against λ and β.

2.1. Wind turbine arrangement with back-to-back PWM-VSCs

In this arrangement both the generator and the grid-side converters are PWM-VSCs as shown in Figure 3. The output voltage of the generator is converted into dc voltage through a PWM-VSC. As the previous model the dc-link voltage is converted to constant frequency voltage using grid side PWM-VSC. The dc-link voltage is controlled by the modulation index (m_a) and power angle (δ). Controlling the dc-link voltage and the bitch angle of the blades of WT will track the maximum power of WT in the case of variable pitch angle control. In the case of fixed pitch angle control the maximum power extraction is achieved by tracking the optimum shaft speed. The grid side PWM-VSC can be used to enhance the stability of the dc-link voltage and controls the active and reactive power from WT by controlling m_a and δ. The generator can be directly controlled by the generator side converter (controller-1) while the grid-side converter (controller-2) maintains the dc-link voltage at the desired value by exporting active power to the grid. Controller-2 also controls the reactive power exchange with the grid [26]. So, the main target of controller-1 is to track the maximum power available from the WTG and the function of controller-2 is to control the dc-link voltage and the reactive power injected to the electric utility.

2.2. Wind turbine arrangement with diode-based rectifier

Figure 4 shows the wind turbine with a diode-based rectifier as the generator-side converter. The diode bridge rectifier converts the generator output ac power to dc power and the PWM-VSC converts the dc power from the rectifier output to ac power. One method to control the operation of the wind turbine with this arrangement (assuming a PMSG) is illustrated in Figure 4. A dc–dc converter is employed to control the dc-link voltage (controller-1), the grid side converter controls the operation of the generator and the power flow to the grid (controller-2). With appropriate control, the generator and turbine speed can be adjusted as wind speed varies so that maximum energy is collected [26]. On the other hand, in most PMSG wind systems,

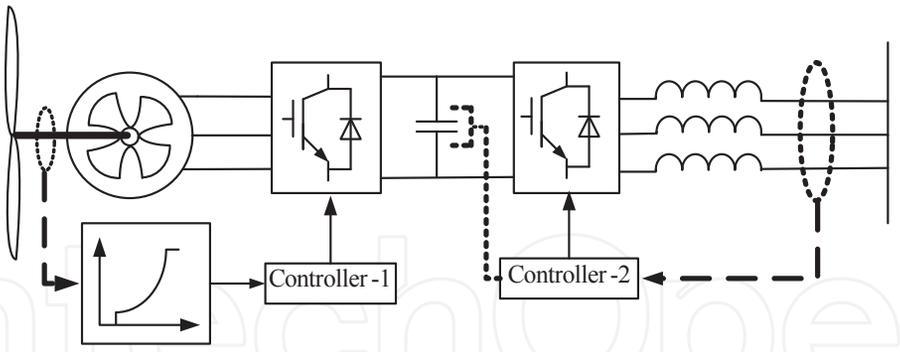

Figure 3. Wind turbine generator with back-to-back PWM-VSCs [26].

the output voltage of the generator is converted into dc voltage via a full-bridge diode rectifier and this dc voltage is adjusted to control the maximum power of turbine. The grid side converter is controlled by grid injected active and reactive power control method. The ac power output from PMSG is fed to a three-phase diode bridge forward by boost converter to effectively control the dc voltage level through the duty ratio of boost converter. The PWM-VSC is used to interface the WTG with the electrical utility also to track the maximum power available from PMSG. The modulation index of the PWM-VSC is controlled to enhance the stability of the dc link voltage as shown in Figure 4.

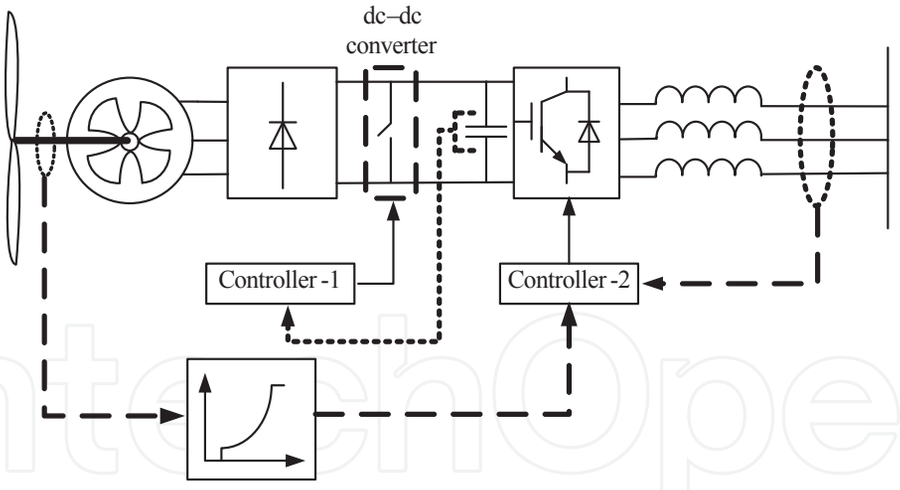

Figure 4. Wind turbine generator with a diode-based rectifier as the generator-side converter [26].

3. MPPT control strategies for the WECS

WECS has been attracting wide attention as a renewable energy source due to depleting fossil fuel reserves and environmental concerns as a direct consequence of using fossil fuel and nuclear energy sources. Wind energy varies continually as wind speed changes throughout

http://dx.doi.org/10.5772/54675

the day, even though abundant. The Amount of power output from a WECS depends upon the accuracy of tracking the peak power points using the MPPT controller irrespective of the generator type used. The maximum power extraction algorithms can be classified into two categories. The two categories are MPPT algorithms with wind speed sensor and MPPT algorithms without wind speed sensor (sensor-less MPPT controller). These two algorithms have been discussed in the following sections.

3.1. MPPT algorithms for a WT with wind speed sensor

3.1.1. Tip Speed Ratio (TSR) technique

The TSR control method regulates the rotational speed of the generator to maintain an optimal TSR at which power extracted is maximum [13]. The target optimum power extracted from wind turbine can be written as [14]:

$$P_{\max} = K_{opt} * \omega_{opt}^3 \tag{5}$$

Where $K_{opt} = 0.5 * \rho A * \left(\frac{r_m}{\lambda_{opt}}\right)^3 * C_{P-\max}$, and $\omega_{opt} = \frac{\lambda_{opt}}{r_m} * u$

The power for a certain wind speed is maximum at a certain value of rotational speed called optimum rotational speed, ω_{opt}. This optimum rotational speed corresponds to optimum tip speed ratio, λ_{opt}. In order to track maximum possible power, the turbine should always operate at λ_{opt}. This is achieved by controlling the rotational speed of the WT so that it always rotates at the optimum rotational speed. As shown in Figure 5, for TSR calculation, both the wind speed and turbine speed need to be measured, and the optimal TSR must be given to the controller. The first barrier to implement TSR control is the wind speed measurement, which adds to system cost and presents difficulties in practical implementations. The second barrier is the need to obtain the optimal value of TSR, this value is different from one system to another. This depends on the turbine-generator characteristics results in custom-designed control software tailored for individual wind turbines [14].

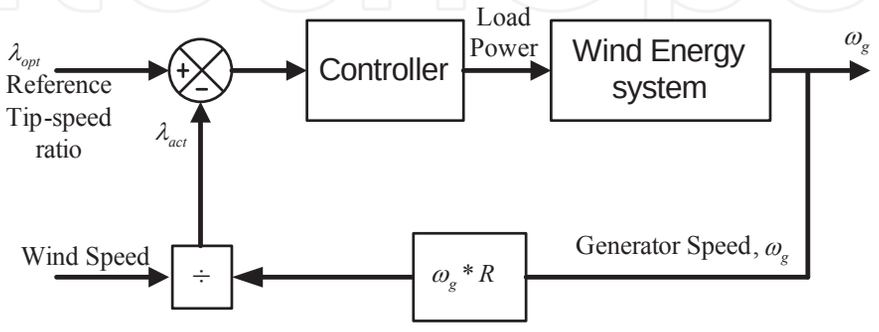

Figure 5. The block diagram of the tip speed ratio control of WECS [15].

3.1.2. Power Signal Feedback (PSF) control

In PSF control [14], it is required to have the knowledge of the wind turbine's maximum power curve, and track this curve through its control mechanisms. The maximum power curves need to be obtained via simulations or off-line experiment on individual wind turbines or from the datasheet of WT which makes it difficult to implement with accuracy in practical applications. In this method, reference power is generated using a maximum power data curve or using the mechanical power equation of the wind turbine where wind speed or the rotational speed is used as the input. Figure 6 shows the block diagram of a WECS with PSF controller for maximum power extraction. The PSF control block generates the optimal power command P_{opt} which is then applied to the grid side converter control system for maximum power extraction as follow [15]:

$$P_{opt} = K_{opt} * \omega_r^{\,3} \tag{6}$$

The actual power output, P_t is compared to the optimal power, P_{opt} and any mismatch is used by the fuzzy logic controller to change the modulation index of the grid side converter, PWM-VSC as shown in Figure 6. The PWM-VSC is used to interface the WT with the electrical utility and will be controlled through the power angle, δ and modulation index, m_a to control the active and reactive power output from the WTG [15].

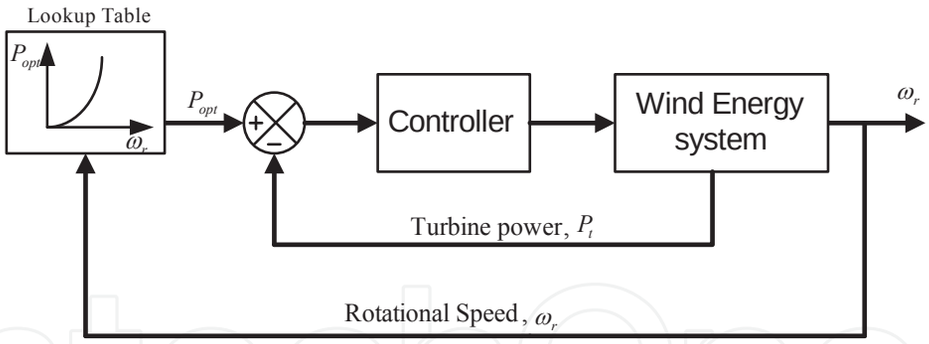

Figure 6. The block diagram of power signal feedback control [15].

3.1.3. Optimal torque control

The aim of the torque controller is to optimize the efficiency of wind energy capture in a wide range of wind velocities, keeping the power generated by the machine equal to the optimal defined value. It can be observed from the block diagram represented in Figure 7, that the idea of this method is to adjust the PMSG torque according to the optimal reference torque of the wind turbine at a given wind speed. A typical wind turbine characteristic with the optimal torque-speed curve plotted to intersect the $C_{P\text{-max}}$ points for each wind speed is illustrated in Figure 8. The curve T_{opt} defines the optimal torque of the device (i.e. maximum energy capture),

http://dx.doi.org/10.5772/54675

and the control objective is to keep the turbine on this curve as the wind speed varies. For any wind speed, the MPPT device imposes a torque reference able to extract the maximum power. The curve T_{opt} is defined by [26]:

$$T_{opt} = K_{opt} * \omega^2_{opt} \tag{7}$$

Where

$$K_{opt} = 0.5 * \rho A * \left(\frac{r_m}{\lambda_{opt}} \right)^3 * C_{P-\max} \tag{8}$$

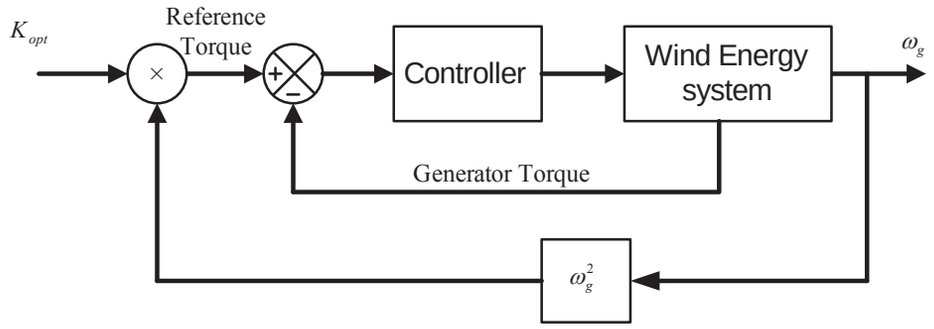

Figure 7. The block diagram of optimal torque control MPPT method.

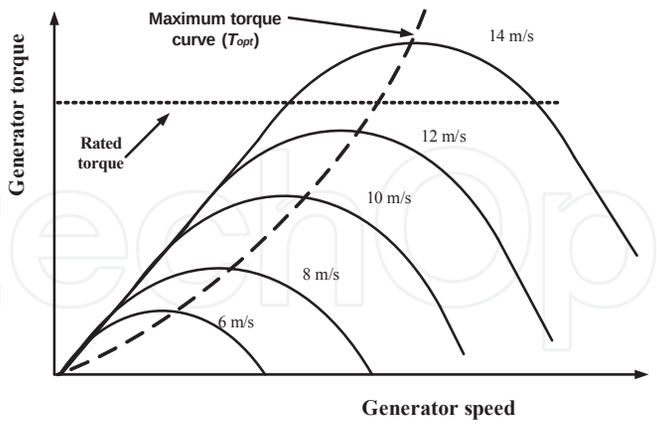

Figure 8. Wind turbine characteristic for maximum power extraction [26].

3.1.4. Load angle control

The load angle control can be explained by analyzing the transfer of active and reactive power between two sources connected by an inductive reactance as shown in Figure 9. The active

power, P_S, and reactive power, Q_S, transferred from the sending-end to the receiving-end can be calculated from the following equation [26]:

$$P_s = \frac{V_s\, V_R}{X_{gen}} \sin\delta \tag{9}$$

$$Q_s = \frac{V_s^2}{X_{gen}} - \frac{V_s\, V_R}{X_{gen}} \tag{10}$$

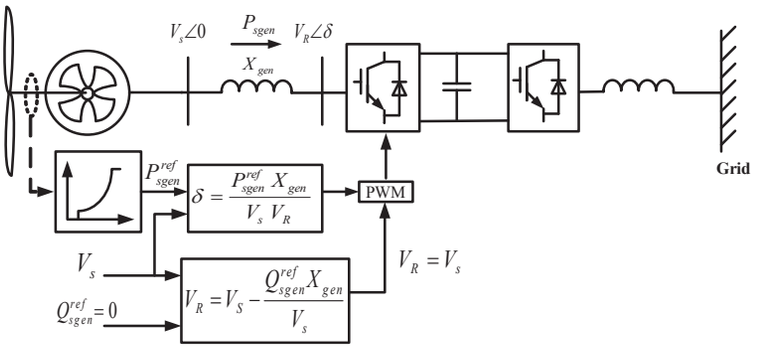

Figure 9. Load angle control of the generator-side converter [26].

3.1.4.1. Load angle control of the generator-side converter

The operation of the generator and the power transferred to the dc-link are controlled by adjusting the magnitude and angle of the voltage at the ac terminals of the generator-side converter. This can be achieved using the load angle control technique where the internal voltage of the generator is the sending source $(V_s\angle 0)$, and the generator-side converter is the receiving source $(V_R\angle\delta)$. The inductive reactance between these two sources is the synchronous reactance of the generator, X_{gen}, as shown in Figure 9 [26].

If it is assumed that the load angle δ is small, then sin $\delta \approx \delta$ and cos $\delta \approx 1$, Then the voltage magnitude, V_R, and angle magnitude, δ, required at the terminals of the generator-side converter are calculated using Equations (7) and (8) as shown [26]:

$$\delta = \frac{P_{Sgen}^{ref} X_{gen}}{V_S V_R} \tag{11}$$

$$V_R = V_S - \frac{Q_{Sgen}^{ref} X_{gen}}{V_S} \tag{12}$$

Where P_{Sgen}^{ref} is the reference value of the active power that needs to be transferred from the generator to the dc-link, and Q_{Sgen}^{ref} is the reference value for the reactive power. The reference value P_{Sgen}^{ref} is obtained from the characteristic curve of the machine for maximum power extraction for a given generator speed, ω_r. As the generator has permanent magnets, it does not require magnetizing current through the stator, thus the reactive power reference value can be set to zero, Q_{Sgen}^{ref}= 0 (i.e. V_S and V_R are equal in magnitude). The implementation of this load angle control scheme is illustrated in Figure 9. The major advantage of the load angle control is its simplicity. However, as the dynamics of the generator are not considered it may not be very effective in controlling the generator during transient operation [26].

3.1.4.2. Load angle control for the grid-side converter

The objective of the grid-side converter controller is to maintain the dc-link voltage at the reference value by exporting active power to the grid. In addition, the controller is designed to enable the exchange of reactive power between the converter and the grid as required by the application specifications. Also, the load angle control is a widely used grid side converter control method, where the grid-side converter is the sending source $(V_S\angle\delta)$, and the grid is the receiving source $(V_R\angle 0)$. As known, the grid voltage is selected as the reference; hence, the phase angle δ is positive. The reactance X_{grid} is the inductor coupling between these two sources [26]. The reference value for the active power, P_{Sgrid}^{ref} , that needs to be transmitted to the grid can be determined by examining the dc-link dynamics with the aid of Figure 10.

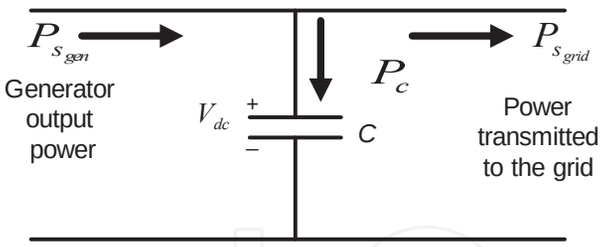

Figure 10. Power flow in the dc-link [26].

This figure illustrates the power balance at the dc-link [26] as shown in the following equation:

$$P_C = P_{Sgen} - P_{Sgrid} \tag{13}$$

where P_C is the power across the dc-link capacitor, C, P_{Sgen} is the active power output of the generator (and transmitted to the dc-link), and P_{Sgrid} is the active power transmitted from the dc-link to the grid.

The dc-link voltage V_{dc} can be expressed in terms of the generator output power, P_{Sgen}, and the power transmitted to the grid, P_{Sgrid}, as shown in the following [26]:

$$V_{dc} = \sqrt{\frac{2}{C}\int \left(P_{Sgen} - P_{Sgrid} \right) dt} \tag{14}$$

Equation (12) calculates the actual value of V_{dc}. The reference value of the active power, P_{Sgrid}^{ref} , to be transmitted to the grid is calculated by comparing the actual dc-link voltage, V_{dc}, with the desired dc-link voltage reference, $V_{dc\text{-}ref}$. The error between these two signals is processed by a PI-controller, whose output provides the reference active power P_{Sgrid}^{ref}, as shown in Figure 11. Figure 12 illustrates the implementation of the load angle control scheme for the grid-side converter with unity power factor [26].

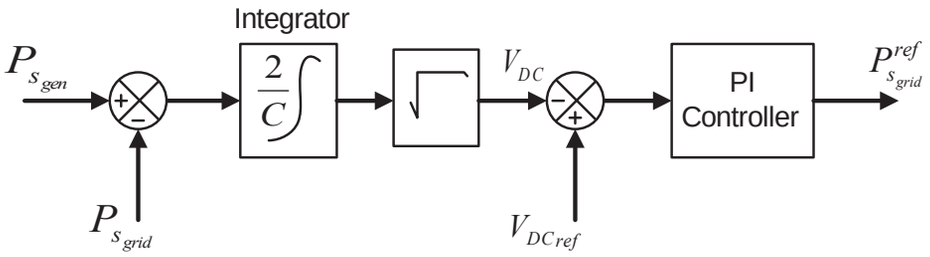

Figure 11. Calculation of active power reference, P_{Sgrid}^{ref} , (suitable for simulation purposes) [26].

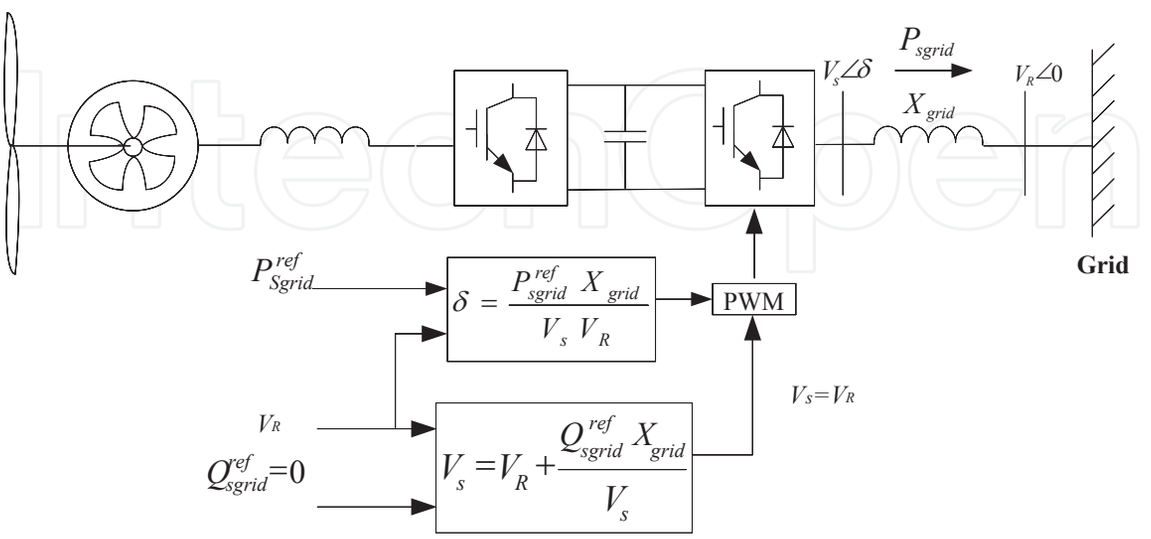

Figure 12. Load angle control of the grid-side converter [26].

http://dx.doi.org/10.5772/54675

3.2. MPPT algorithms for a WT without wind speed sensor

3.2.1. Hill-Climb Searching (HCS)

3.2.1.1. Principle of Hill-Climb Searching (HCS)

The HCS [11], control algorithm continuously searches for the peak power of the wind turbine. The maximum power can be extracted from WTG without requiring information about the wind and generator speeds (Hill-Climb Searching, HCS) [1, 11]. It can overcome some of the common problems normally associated with the other two methods, TSR and PSF. The tracking algorithm depends on the location of the operating point. According to the changes in power and speed the desired optimum signal has been computed in order to track the point of maximum power. Figure 13 shows the principle of HCS control where the operating point is moving toward or away from the maximum turbine power according to increasing (down-hill region) or decreasing the dc current, I_{dm} (up-hill region). The down-hill and up-hill regions are named according to the trend of the system output power with respect to the inverter dc-link voltage, V_{dc} for a wind energy system. If an increase of I_{dm} leads to an increase of the system output power, the HCS method considers the turbine running in the down-hill region, and I_{dm} should keep increasing toward the maximum power point; otherwise, the turbine is considered as running in the up-hill region, and I_{dm} decreasing will be the choice of the HCS method towrds the maximum power point [11].

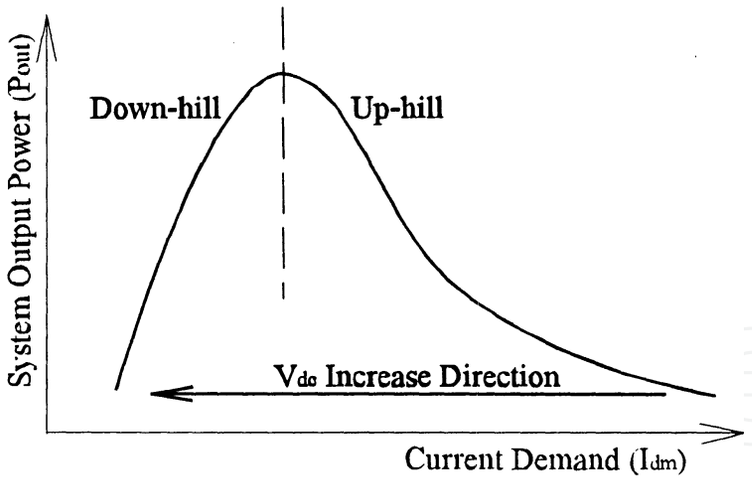

Figure 13. HCS control principle [11].

3.2.1.2. Advanced Hill-Climb Searching (HCS) method

Reference [11] introduces an advanced hill climb searching, AHCS which has been proposed to maximize P_m, through detecting the inverter output power and inverter dc-link voltage. The authors use a diode rectifier to convert the three-phase output ac voltage of a generator to V_{dc} as shown in Figure 14.

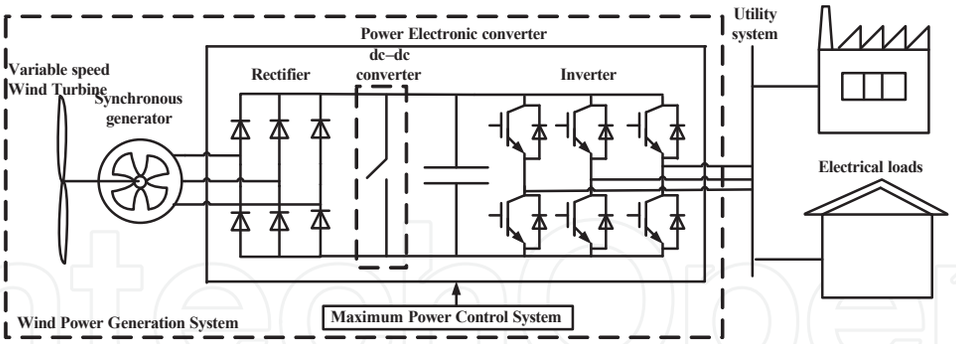

Figure 14. Typical wind power generation system connected to a utility grid [11].

V_{dc} is related to the generator angular rotational speed (ω_r) by a function of the generator field current (I_f) and the load current (I_g) as shown [11]:

$$V_{dc} = k(I_f, I_g) * \omega_r \tag{15}$$

The algorithm uses the relationship between the turbine mechanical power (P_m), and the electrical system output power (P_{out}) given by Equation (14). By differentiating Equation (14) to get a relationship for ΔP_m, Equation (15) is obtained:

$$P_m = P_{load} + T_f * \omega_r + \omega_r * J\frac{d\omega_r}{dt} = \frac{P_{out}}{\eta} + T_f * \omega_r + \omega_r * J\frac{d\omega_r}{dt} \tag{16}$$

$$\Delta P_m = \frac{\Delta P_{out}}{\eta} + T_f * \Delta\omega_r + \Delta(\omega_r * J\frac{d\omega_r}{dt}) \tag{17}$$

Authors noted that if the sampling period of the control system is adequately small then the term $k(I_f, I_g)$ can be considered as a constant value k during a sampling period. $T_f * \omega$ and η can also be considered as constant values in the same sampling period. Based on the above assumptions, Equation (15) leads to Equation (16) for digital control purposes.

$$\Delta P_m = \frac{\Delta P_{out}}{\eta} + JK^2 * \Delta(V_{dc} * \frac{dV_{dc}}{dt}) \tag{18}$$

In order to establish rules to adjust the system's operating point, this method evaluates the values of ΔP_{out} and $\Delta(V_{dc} * dV_{dc}/dt)$ (which represents $\Delta(\omega_r * d\omega_r/dt)$) based on Equation (14). Depending on the values of ΔP_{out} and $\Delta(V_{dc} * dV_{dc}/dt)$ the polarity of the inverter current demand control signal (I_{dm}) is decided according to Equation (16). There are three basic modes for this method, i) initial mode, ii) training mode, and iii) application mode as shown in Figure 15.

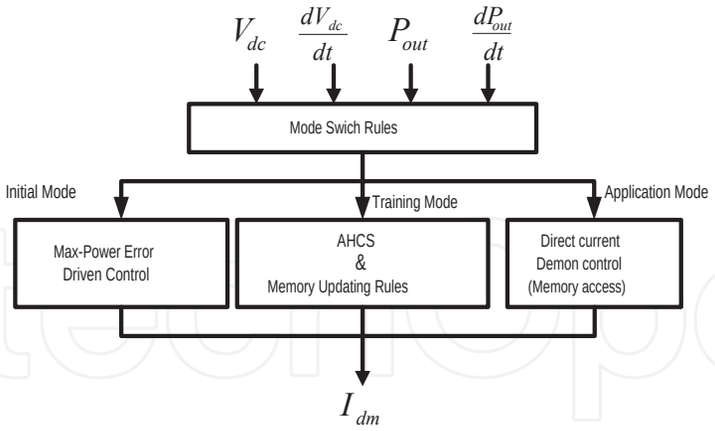

Figure 15. Structure of the intelligent maximum wind power extraction algorithm [11].

During its initial mode, before the algorithm has been trained, the magnitude of I_{dm} is determined by the maximum power error driven (MPED) control. MPED control is the implementation of the conventional HCS method in terms of wind energy system characteristics. During its training mode, the algorithm continually records and updates operating parameters into its programmable lookup table for its intelligent memory feature. Since this method is trainable with its intelligent memory, it allows itself to adapt to work with different WT. As a result, it is a solution to the customization problems of many algorithms. Another advantage of this algorithm is that it does not require mechanical sensors (like anemometers) which lowers its cost and eliminates its associated practical problems. However, it can be seen in [11] that the algorithm is relatively slow and complex as it has three different modes of operation. Another drawback is that the algorithm cannot take into account of the changes in air density, which affects the power characteristics quite significantly.

3.2.2. MPPT algorithm by directly adjusting the DC/DC converter duty cycle and modulation index of the PWM-VSC

MPPT Algorithm by Directly Adjusting the dc/dc Converter duty ratio, *D*, and Modulation Index of the PWM-VSC, m_a, is shown in Figure 16. In this direct drive converter, the mechanical power from the WT model is fed to the PMSG. The three-phase output voltages of the PMSG are fed to the three- phase diode bridge rectifier. There is no control on the output voltage of the diode bridge rectifier so it cannot be connected directly to the PWM because the PWM inverter needs constant dc voltage. So, a dc/dc converter should be used to control the dc-link voltage. Depending on the dc output voltage required from the dc/dc converter, boost or buck converter can be used. In this study, the dc output voltage, $V_{d,out}$ is required to be higher than input dc voltage, $V_{d,in,}$ so the boost converter is used. By controlling the dc voltage to be constant by controlling of D the boost converter and m_a the maximum available power from the wind can be extracted. The main drawback of this system is the diode bridge and boost converter are unidirectional power flow devices, so the PMSG has to work only in generator mode which may affect the stability of the system at abnormal conditions. A high capacitance of the dc link capacitor can remedy the effects of this drawback [18].

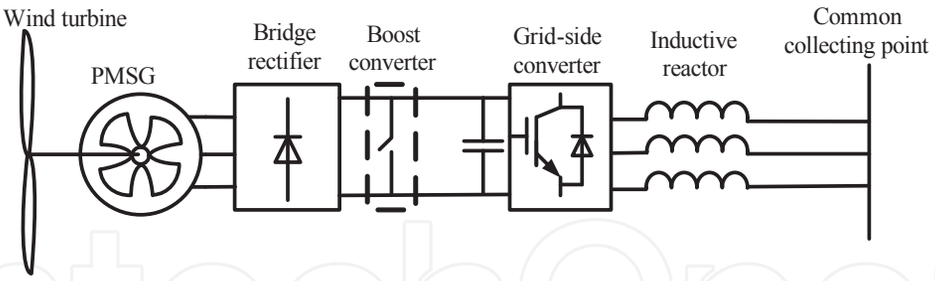

Figure 16. Modelling of wind turbine driving permanent magnet synchronous generator.

The active and reactive power can be obtained in terms of m_a and D of the boost converter as shown in Equation (17) and Equation (18), respectively [18].

$$P_{out} = \frac{\sqrt{3}\, m_a V_{d,in} V_{LLU} * \sin\delta}{2\sqrt{2}\,(1-D)X_s} \tag{19}$$

$$Q_{out} = \frac{\sqrt{3}\, m_a V_{d,in}}{2\sqrt{2}\,(1-D)X_s}\left(V_{LLU} * \cos\delta - \frac{\sqrt{3}\, m_a V_{d,in}}{2\sqrt{2}\,(1-D)} \right) \tag{20}$$

Where;

δ: torque angle at the electric utility side.

X_s: synchronous reactance of the electric utility.

It is clear from Equation (17) and Equation (18) that the active and reactive power can be controlled by controlling modulation index, m_a of the PWM inverter and duty ratio of the boost converter.

3.2.3. Maximum power extraction and reactive power technique

3.2.3.1. Decoupled control of the active and reactive power, dependently

This method presents an algorithm for maximum power extraction and reactive power control of an inverter based variable-speed wind-turbine generator without wind speed sensor. The algorithm does not require information about the wind and generator speeds or the inverter dc-link voltage and thus, is dependent of specifications of the wind turbine generation system [1].

Consider the wind-turbine generation system of Figure 17. The turbine mechanical power P_m and the generator output power P_g are related by

$$P_m = Pg + \omega_r * J\frac{d\omega_r}{dt} = \frac{P_{out}}{\eta} + \omega_r * J\frac{d\omega_r}{dt} \tag{21}$$

where P_{out} is the converter output power, ω_r is the generator speed, J is the combined turbine and generator moment of inertia and η is the overall system efficiency.

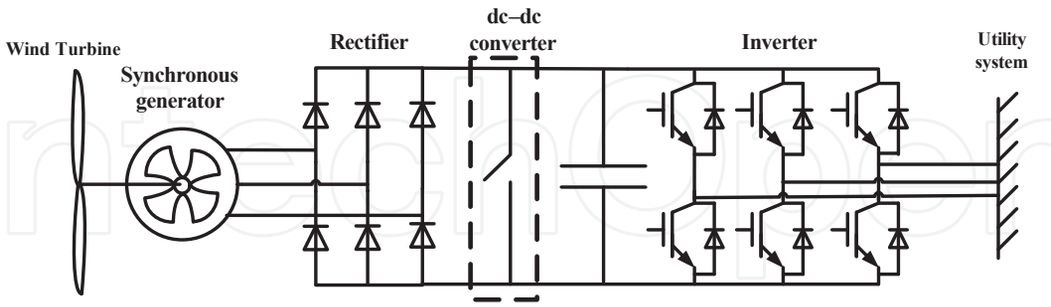

Figure 17. Grid-connected wind-turbine generation system [1].

A. Real power

This part shows how a maximum power can be extracted from a WTG without requiring information about the wind and generator speeds. In the system of Figure 17, the converter dc-link voltage is proportional to the generator speed, $V_{dc} = K\omega_r$, since the generator terminal voltage is proportional to the speed. Thus, Equation (19) can be expressed in terms of V_{dc} as [1]:

$$P_m = \frac{P_{out}}{\eta} + \frac{J}{K^2} V_{dc} \frac{dV_{dc}}{dt} \tag{22}$$

Taking the derivative of Equation (20), we deduce

$$\Delta P_m = \frac{\Delta P_{out}}{\eta} + \frac{J}{K^2} \Delta(V_{dc} \frac{dV_{dc}}{dt}) \tag{23}$$

V_{dc} is proportional to the inverter terminal voltage V_{inv} divided by the inverter amplitude modulation index, m_a. Thus, $\Delta V_{dc} = \Delta(V_{inv}/m_a)$. To extract maximum power from the wind, a small perturbation is applied to the angle of the inverter terminal voltage, δ. ΔP_{out} and $\Delta(V_{inv}/m_a)$ are estimated and their signs determine whether the operating point is moving toward or away from the maximum turbine power, Figure 18. Depending on the operating point direction of movement, the decision is to increase or decrease the angle δ or to keep it constant. Table 1 describes the decision that is made based on the sign of the inverter output power variation ΔP_{out} and that of the ratio of the inverter terminal voltage to the amplitude modulation index $\Delta(V_{inv}/m_a)$. With the proposed algorithm for maximum power extraction, only voltage and current at the inverter terminal need to be measured, and no information about the wind and generator speeds and the dc-link voltage is required [1].

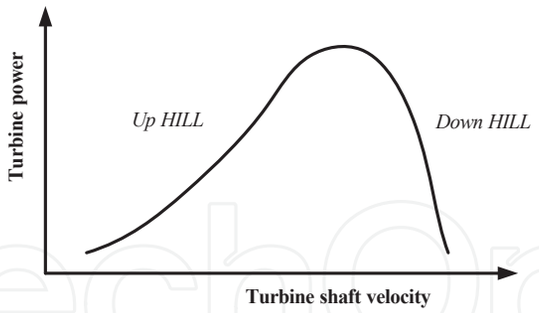

Figure 18. Wind turbine output power versus speed [1].

ΔP_{out}	$\Delta(\frac{V_{inv}}{m_a})$	Decision
> 0	> 0	Increase δ
< 0	< 0	Decrease δ
> 0	< 0	No change
< 0	> 0	No change

Table 1. Maximum power tracking algorithm [1].

B. Reactive power

The inverter should be able to regulate its output reactive power to provide the reactive power demand of the utility system, Figure 17. The inverter output reactive power must be controlled so as the maximum real power extraction is not violated. The real and reactive power components (P_{out}, Q_{out}) at the inverter output terminals are [1]:

$$P_{out} = \frac{V_{inv} V_{sys}}{X_T} \sin(\delta) \tag{24}$$

$$Q_{out} = \frac{V_{inv} V_{sys}}{X_T} \cos(\delta) - \frac{\left(V_{sys}\right)^2}{X_T} \tag{25}$$

V_{sys} is the utility system voltage and X_T is the reactance between the inverter and the utility system. It is seen from Equation (22) and Equation (23) that V_{inv} and δ can be controlled so as Q_{out} is regulated at a desired value while P_{out} is kept constant at its maximum corresponding to the wind speed. Substituting V_{inv} in Equation (22) by $\frac{\sqrt{3}}{2\sqrt{2}}\ m_a\ V_d$, This equation can be deduced as follow:

http://dx.doi.org/10.5772/54675

$$P_{out} = \frac{\sqrt{3}\ m_a V_{dc} V_{sys}}{2\sqrt{2}X_T}\sin(\delta) \tag{26}$$

Assuming that V_{dc} does not change over the small sampling period T, P_{out} corresponding to the sampling time nT and $(n+1)T$ is

$$P_{out(n)} = \frac{\sqrt{3}\, m_{a(n)} V_{dc} V_{sys}}{2\sqrt{2}\, X_T}\sin(\delta_n) \tag{27}$$

$$P_{out(n+1)} = \frac{\sqrt{3}\, m_{a(n+1)} V_{dc} V_{sys}}{2\sqrt{2}\, X_T}\sin(\delta_{n+1}) \tag{28}$$

To keep the real power constant, i.e., $P_{out\,(n+1)} = P_{out\,(n)}$, while providing a desired reactive power, Equation (23), the inverter voltage angle must satisfy the following condition.

$$\delta_{n+1} = \sin^{-1}\left[\frac{m_{a(n)}}{m_{a(n+1)}}\sin(\delta_n)\right] \tag{29}$$

Figure 19 shows a flowchart of the proposed algorithm for maximum power extraction and reactive power control of a wind-turbine generator. The inputs are the three-phase voltages and currents at the inverter output terminals and the outputs are the required amplitude modulation index and the voltage angle of the inverter.

3.2.3.2 Decoupled control of the active and reactive power, independently

In this study [17], simple ac-dc-ac power conversion system and proposed modular control strategy for grid-connected wind power generation system have been implemented. Grid-side inverter maintains the dc-link voltage constant and the power factor of line side can be adjusted. Input current reference of dc/dc boost converter is decided for the maximum power point tracking of the turbine without any information of wind or generator speed. As the proposed control algorithm does not require any speed sensor for wind or generator speed, construction and installation are simple, cheap, and reliable. The main circuit and control block diagrams are shown in Figure 20. For wide range of variable speed operation, a dc-dc boost converter is utilized between 3-phase diode rectifier and PWM-VSC. The input dc current is regulated to follow the optimized current reference for maximum power point operation of turbine system. Grid PWM-VSC supply currents into the utility line by regulating the dc-link voltage. The active power is controlled by q-axis current through regulating the dc-link voltage whereas the reactive power can be controlled by d-axis current via adjusting the power factor

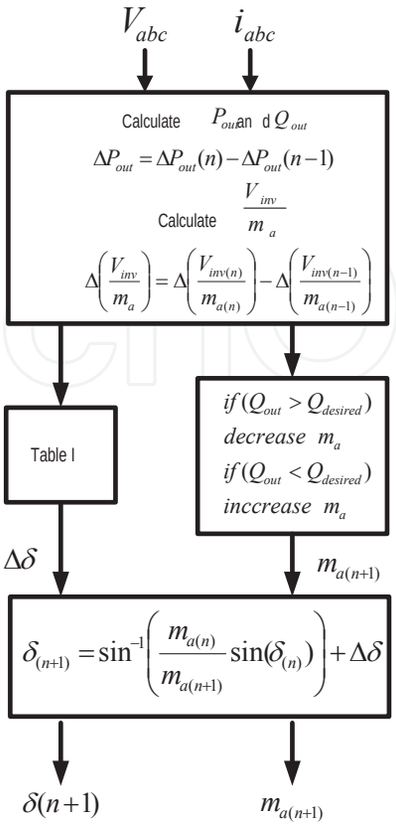

Figure 19. Flowchart of the proposed maximum active power and reactive power control [1].

of the grid side converter as shown in Figure 20. The phase angle of utility voltage is detected using Phased Locked Loop, *PLL*, in d-q synchronous reference frame [17].

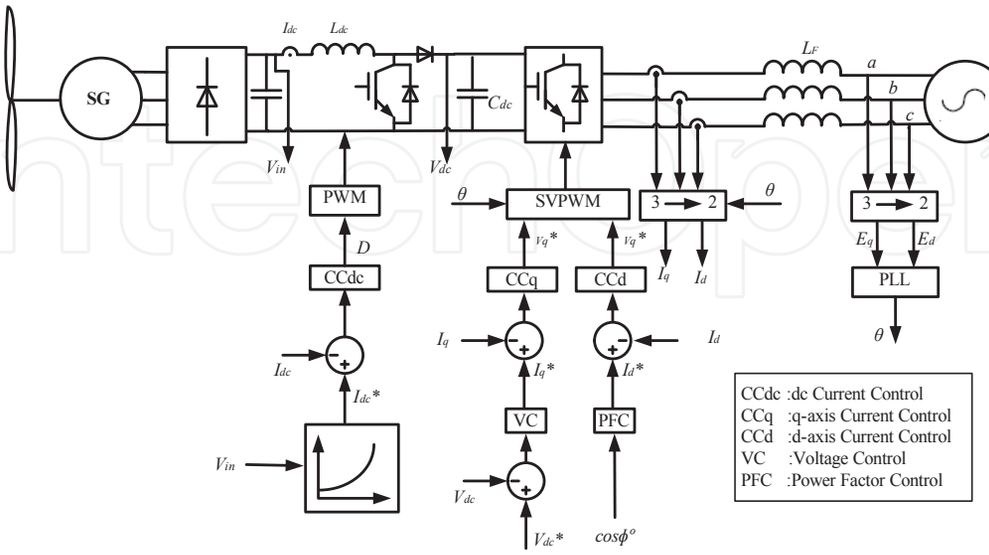

Figure 20. Block diagram of system control [17].

http://dx.doi.org/10.5772/54675

4. Co-simulation (PSIM/Matlab) program for interconnecting wind energy system with electric utility

In this study, the WECS is designed as PMSG connected to the grid via a back-to-back PWM-VSC as shown in Figure 21. MPPT control algorithm has been introduced using FLC to regulate the rotational speed to force the PMSG to work around its maximum power point in speeds below rated speeds and to produce the rated power in wind speed higher than the rated wind speed of the WT. Indirect vector-controlled PMSG system has been used for this purpose. The input to FLC is two real time measurements which are the change of output power and rotational speed between two consequent iterations (ΔP, and $\Delta\omega_m$). The output from FLC is the required change in the rotational speed $\Delta\omega_{m\text{-}new}$*. The detailed logic behind the new proposed technique is explained in details in the following sections. Two effective computer simulation software packages (PSIM and Simulink) have been used to carry out the simulation effectively where PSIM contains the power circuit of the WECS and Matlab/Simulink contains the control circuit of the system. The idea behind using these two different software packages is the effective tools provided with PSIM for power circuit and the effective tools in Simulink for control circuit and FLC.

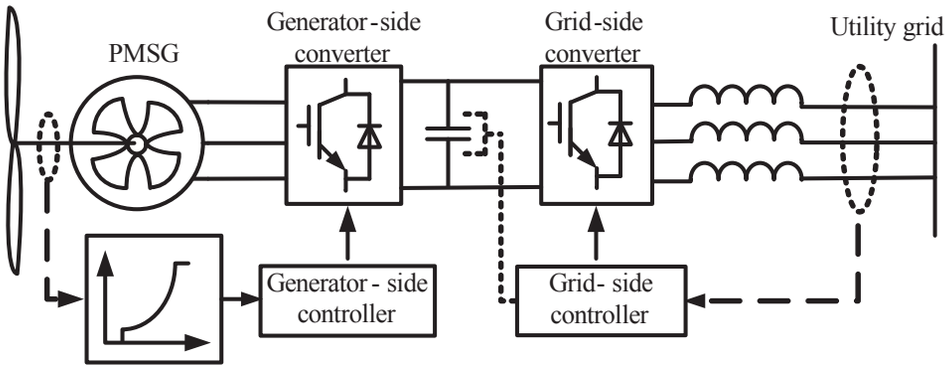

Figure 21. Schematic diagram of the overall system.

4.1. Wind energy conversion system description

Figure 22 shows a co-simulation (PSIM/Simulink) program for interconnecting WECS to electric utility. The PSIM program contains the power circuit of the WECS and Matlab/Simulink program contains the control of this system. The interconnection between PSIM and Matlab/Simulink has been done via the SimCoupler block. The basic topology of the power circuit which has PMSG driven wind turbine connected to the utility grid through the ac-dc-ac conversion system is shown in Figure 21. The PMSG is connected to the grid through back–to-back bidirectional PWM voltage source converters VSC. The generator side converter is used as a rectifier, while the grid side converter is used as an inverter. The generator side converter is connected to the grid side converter through dc-link capacitor. The control of the overall system has been done through the generator side converter and the grid side converter.

MPPT algorithm has been achieved through controlling the generator side converter using FLC. The grid-side converter controller maintains the dc-link voltage at the desired value by exporting active power to the grid and it controls the reactive power exchange with the grid.

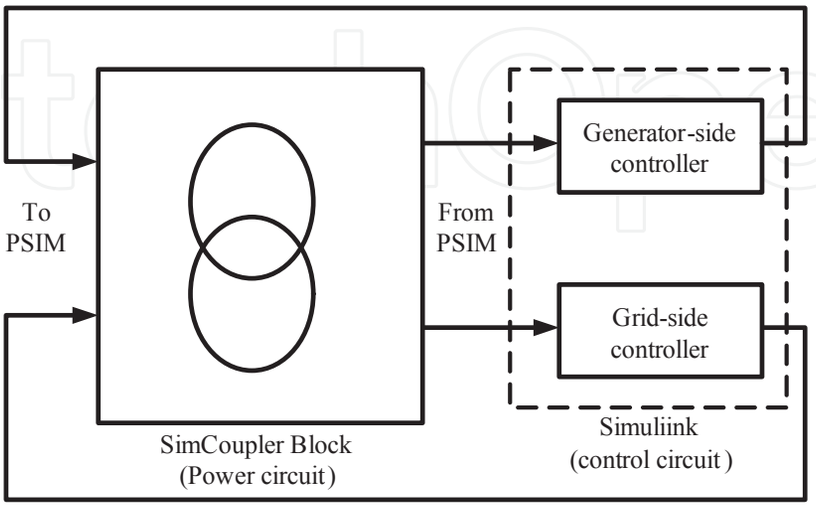

Figure 22. Co-simulation block of wind energy system interfaced to electric utility.

4.1.1. Wind turbine model

Wind turbine converts the wind power to a mechanical power. This mechanical power generated by wind turbine at the shaft of the generator can be expressed as:

$$P_m = \frac{1}{2} C_P(\lambda, \beta) \rho A u^3 \tag{30}$$

where ρ is the air density (typically 1.225 kg/m^3), β is the pitch angle (in degree), A is the area swept by the rotor blades (in m^2); u is the wind speed (in m/s) and $C_p(\lambda, \beta)$ is the wind-turbine power coefficient (dimensionless).

The turbine power coefficient, $C_p(\lambda, \beta)$, describes the power extraction efficiency of the WT and is defined as the ratio between the mechanical power available at the turbine shaft and the power available in wind. A generic equation shown later in Equation (3) is used to model $C_p(\lambda, \beta)$. C_P is a nonlinear function of both tip speed ratio, λ and the blade pitch angle, β. The tip speed ratio, λ is the ratio of the turbine tip speed, ω_m*R to the wind speed, u. This tip speed ratio, λ, is defined as [28]:

$$\lambda = \frac{\omega_m * R}{u} \tag{31}$$

Where ω_m is the rotational speed and R is the turbine blade radius, respectively.

http://dx.doi.org/10.5772/54675

For a fixed pitch angle, β, C_P becomes a nonlinear function of tip speed ratio, λ, only. According to Equation (29), there is a relation between the tip speed ratio, λ and the rotational speed, ω_m. Hence, at a certain wind speed, the power is maximum at a certain ω_m called optimum rotational speed, ω_{opt}. This speed corresponds to optimum TSR, λ_{opt} [15]. The value of the TSR is constant for all maximum power points. So, to extract maximum power at variable wind speed, the WT should always operate at λ_{opt} in speeds bellow the rated speed. This occurs by controlling the rotational speed of the WT to be equal to the optimum rotational speed. Figure 23 shows that the mechanical power generated by WT at the shaft of the generator as a function of the rotational speed, ω_m. These curves have been extracted from PSIM support for the wind turbine used in this study. It is clear from this figure that for each wind speed the mechanical output power is maximum at particular rotational speed, ω_{opt} as shown in Figure 23.

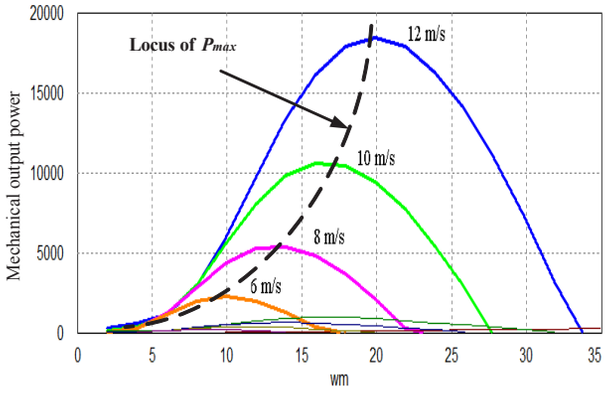

Figure 23. Typical output power characteristics.

4.1.2. PMSG model

The generator is modeled by the following voltage equations in the rotor reference frame (dq axes) [29]:

$$v_{sd} = R_s i_{sd} + \frac{d\lambda_{sd}}{dt} - \omega_r \lambda_{sq}$$
$$v_{sq} = R_s i_{sq} + \frac{d\lambda_{sq}}{dt} + \omega_r \lambda_{sd} \quad (32)$$

Where λ_{sq}, and λ_{sd} are the stator flux linkages in the direct and quadrature axis of rotor which in the absence of damper circuits can be expressed in terms of the stator currents and the magnetic flux as [29].

$$\lambda_{sd} = L_s i_{sd} + \psi_F$$
$$\lambda_{sq} = L_s i_{sq} \quad (33)$$

Where ψ_F is the flux of the permanent magnets.

The electrical torque T_e of the three-phase generator can be calculated as follows [29, 30]:

$$T_e = \frac{3}{2} P \left[\lambda_{sd} i_{sq} - \lambda_{sq} i_{sd}\right] \tag{34}$$

Where P is the number of pole pairs. For a non-salient-pole machine the stator inductances L_{sd} and L_{sq} are approximately equal. This means that the direct-axis current i_{sd} does not contribute to the electrical torque. Our concept is to keep i_{sd} to zero in order to obtain maximal torque with minimum current. Then, the electromagnetic torque results:

$$T_e = \frac{3}{2} P \psi_F i_{sq} = K_c i_{sq} \tag{35}$$

K_c is called the torque constant and represents the proportional coefficient between T_e and i_{sq}.

4.2. Control of the generator side converter (PMSG)

The generator side controller controls the rotational speed to produce the maximum output power via controlling the electromagnetic torque according to Equation (33), where the indirect vector control is used. The proposed control logic of the generator side converter is shown in Figure 24. The speed loop will generate the q-axis current component to control the generator torque and speed at different wind speed via estimating the references value of i_α, i_β as shown in Figure 24. The torque control can be achieved through the control of the i_{sq} current as shown in Equation (33). Figure 25 shows the stator and rotor current space phasors and the excitation flux of the PMSG. The quadrature stator current i_{sq} can be controlled through the rotor reference frame (α, β axis) as shown in Figure 25. So, the references value of i_α, i_β can be estimated easily from the amplitude of i_{sq^*} and the rotor angle, Θ_r. Initially, to find the rotor angle, Θ_r, the relationship between the electrical angular speed, ω_r and the rotor mechanical speed (rad/sec), ω_m may be expressed as:

$$\omega_r = \frac{P}{2} \omega_m \tag{36}$$

So, the rotor angle, Θ_r, can be estimated by integrating of the electrical angular speed, ω_r. The input to the speed control is the actual and reference rotor mechanical speed (rad/sec) and the output is the (α, β) reference current components. The actual values of the (α, β) current components are estimated using Clark's transformation to the three phase current of PMSG. The FLC can be used to find the reference speed along which tracks the maximum power point.

http://dx.doi.org/10.5772/54675

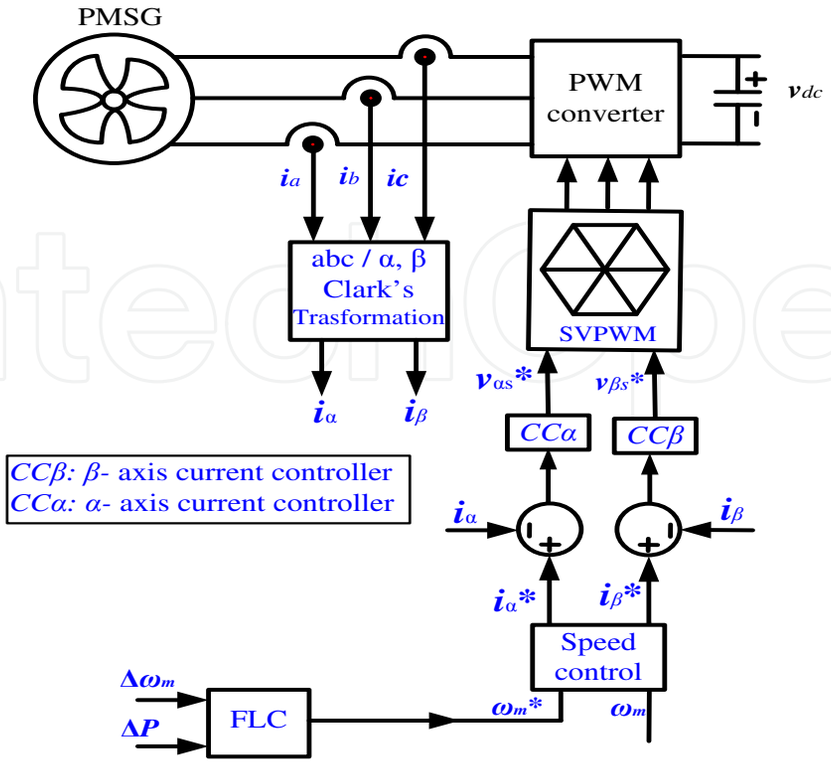

Figure 24. Control block diagram of generator side converter.

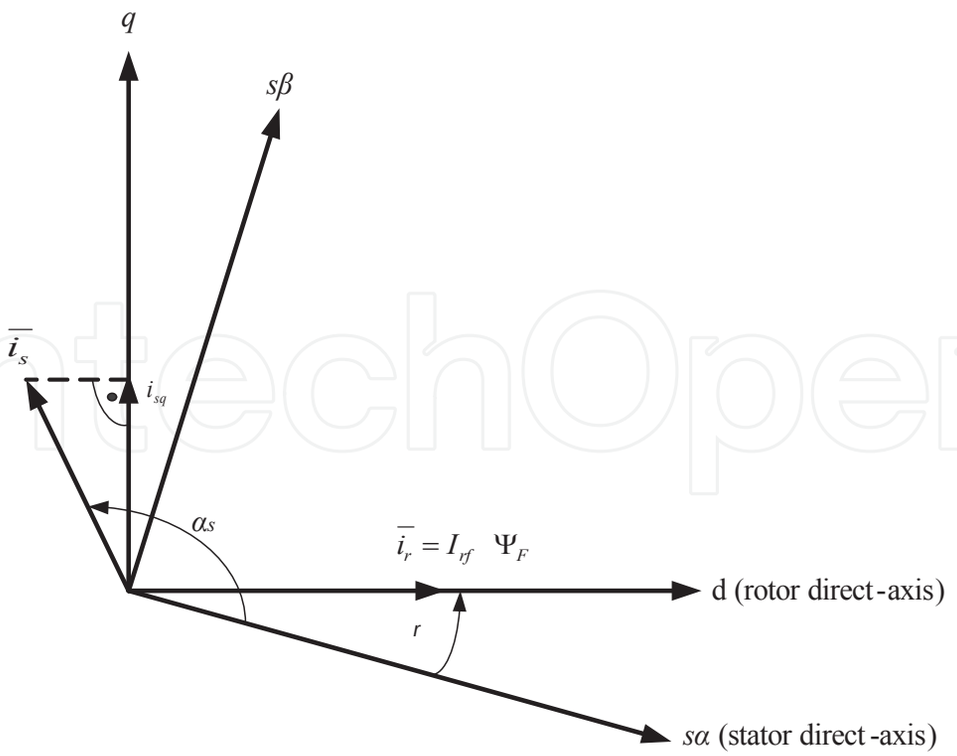

Figure 25. The stator and rotor current space phasors and the excitation flux of the PMSG [29].

4.3. Fuzzy logic controller for MPPT

At a certain wind speed, the power is maximum at a certain ω called optimum rotational speed, ω_{opt}. This speed corresponds to optimum tip speed ratio, λ_{opt} [15]. So, to extract maximum power at variable wind speed, the turbine should always operate at λ_{opt}. This occurs by controlling the rotational speed of the turbine. Controlling of the turbine to operate at optimum rotational speed can be done using the fuzzy logic controller. Each wind turbine has one value of λ_{opt} at variable speed but ω_{opt} changes from a certain wind speed to another. From Equation (29), the relation between ω_{opt} and wind speed, u, for constant R and λ_{opt} can be deduced as follow:

$$\omega_{opt} = \frac{\lambda_{opt}}{R} u \tag{37}$$

From Equation (35), the relation between the optimum rotational speed and wind speed is linear. At a certain wind speed, there is optimum rotational speed which is different at another wind speed. The fuzzy logic control is used to search (observation and perturbation) the rotational speed reference which tracks the maximum power point at variable wind speeds. The fuzzy logic controller block diagram is shown in Figure 26. Two real time measurements are used as input to fuzzy (ΔP, and $\Delta\omega_m$*) and the output is ($\Delta\omega_{m\text{-}new}$*). Membership functions are shown in Figure 27. Triangular symmetrical membership functions are suitable for the input and output, which give more sensitivity especially as variables approach to zero value. The width of variation can be adjusted according to the system parameter. The input signals are first fuzzified and expressed in fuzzy set notation using linguistic labels which are characterized by membership functions before it is processed by the FLC. Using a set of rules and a fuzzy set theory, the output of the FLC is obtained [22]. This output, expressed as a fuzzy set using linguistic labels characterized by membership functions, is defuzzified and then produces the controller output. The fuzzy logic controller doesn't require any detailed mathematical model of the system and its operation is governed simply by a set of rules. The principle of the fuzzy logic controller is to perturb the reference speed ω_m* and to observe the corresponding change of power, ΔP. If the output power increases with the last increment, the searching process continues in the same direction. On the other hand, if the speed increment reduces the output power, the direction of the searching is reversed. The fuzzy logic controller is efficient to track the maximum power point, especially in case of frequently changing wind conditions [22].

Figure 27 shows the input and output membership functions and Table 2 lists the control rule for the input and output variable. The next fuzzy levels are chosen for controlling the inputs and output of the fuzzy logic controller. The variation step of the power and the reference speed may vary depending on the system. In Figure 27, the variation step in the speed reference is from -0.15rad/s to 0.15rad/s for power variation ranging over from -30W to 30W. The membership definitions are given as follows: N (negative), N++ (very big negative), NB (negative big), NM (negative medium), NS (negative small), ZE (zero), P (positive), PS (positive small), PM (positive medium), PB (positive big), and P++ (very big positive).

http://dx.doi.org/10.5772/54675

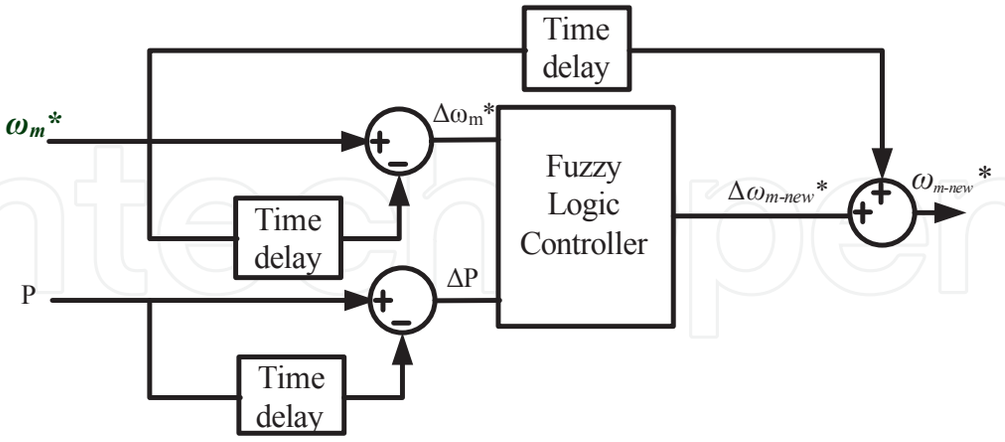

Figure 26. Input and output of fuzzy controller.

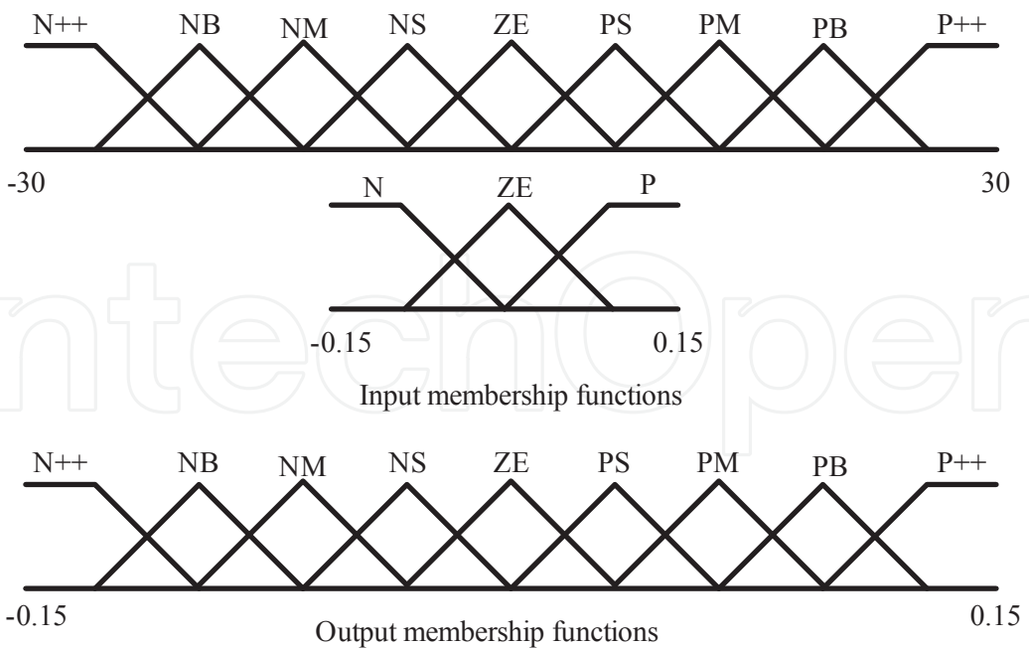

Figure 27. Membership functions of fuzzy logic controller

ΔP / $\Delta\omega_m$	**N++**	**NB**	**NM**	**NS**	**ZE**	**PS**	**PM**	**PB**	**P++**
N	P++	PB	PM	PS	ZE	NS	NM	NB	N++
ZE	NB	NM	NS	NS	ZE	PS	PM	PM	PB
P	N++	NB	NM	NS	ZE	PM	PM	PB	PB

Table 2. Rules of fuzzy logic controller

4.4. Control of the grid side converter

The power flow of the grid-side converter is controlled in order to maintain the dc-link voltage at reference value, 600v. Since increasing the output power than the input power to dc-link capacitor causes a decrease of the dc-link voltage and vise versa, the output power will be regulated to keep dc-link voltage approximately constant. To maintain the dc-link voltage constant and to ensure the reactive power flowing into the grid, the grid side converter currents are controlled using the d-q vector control approach. The dc-link voltage is controlled to the desired value by using a PI-controller and the change in the dc-link voltage represents a change in the q-axis (i_{qs}) current component. Figure 28 shows a control block diagram of the grid side converter.

The active power can be defined as;

$$P_s = \frac{3}{2}\left(v_{ds}i_{ds} + v_{qs}i_{qs}\right) \tag{38}$$

The reactive power can be defined as:

$$Q_s = \frac{3}{2}\left(v_{qs}i_{ds} - v_{ds}i_{qs}\right) \tag{39}$$

By aligning the q-axis of the reference frame along with the grid voltage position v_{ds}=0 and v_{qs}= constant because the grid voltage is assumed to be constant. Then the active and reactive power can be obtained from the following equations:

$$P_s = \frac{3}{2}v_{qs}i_{qs} \tag{40}$$

$$Q_s = \frac{3}{2}v_{qs}i_{ds} \tag{41}$$

http://dx.doi.org/10.5772/54675

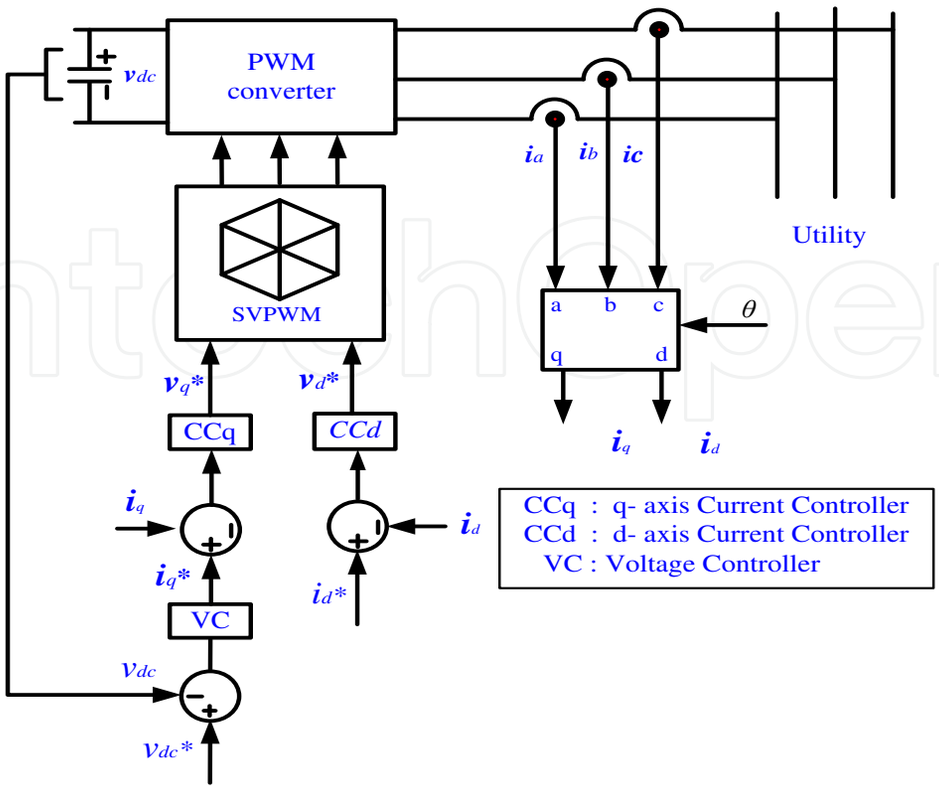

Figure 28. Control block diagram of grid-side converter.

4.5. Simulation results

A co-simulation (PSIM/Simulink) program has been used where PSIM contains the power circuit of the WECS and Matlab/Simulink has the whole control system as described before. The model of WECS in PSIM contains the WT connected to the utility grid through back–to-back bidirectional PWM converter. The control of whole system in Simulink contains the generator side controller and the grid side controller. The wind turbine characteristics and the parameters of the PMSG are listed in Appendix. The generator can be directly controlled by the generator side controller to track the maximum power available from the WT. The wind speed is variable and changes from 7 m/s to 13 m/s as input to WT. To extract maximum power at variable wind speed, the turbine should always operate at λ_{opt}. This occurs by controlling the rotational speed of the WT. So, it always operates at the optimum rotational speed. ω_{opt} changes from a certain wind speed to another. The fuzzy logic controller is used to search the optimum rotational speed which tracks the maximum power point at variable wind speeds. Figure 29 (a) shows the variation of the wind speed which varies randomly from 7 m/s to13 m/s. On the other hand, Figure 29 (b) shows the variation of the actual and reference rotational speed as a result of the wind speed variation. At a certain wind speed, the actual and reference rotational speed have been estimated and this agree with the power characteristic of the wind turbine shown later in Figure 23. I.e. the WT always operates at the optimum rotational speed which is found using FLC; hence, the power extraction from wind is maximum at variable

wind speed. It is seen that according to the wind speed variation the generator speed varies and that its output power is produced corresponding to the wind speed variation. The fuzzy logic controller works well and it gives the good tracking performance for the maximum output power point. The fuzzy logic controller makes WT always operates at the optimum rotational speed. On the other hand, the grid-side controller maintains the dc-link voltage at the desired value, 600v, as shown in Figure 29 (c). The dc-link voltage is regulated by exporting active power to the grid as shown in Figure 29 (d). The reactive power transmitted to the grid is shown in Figure 29 (e).

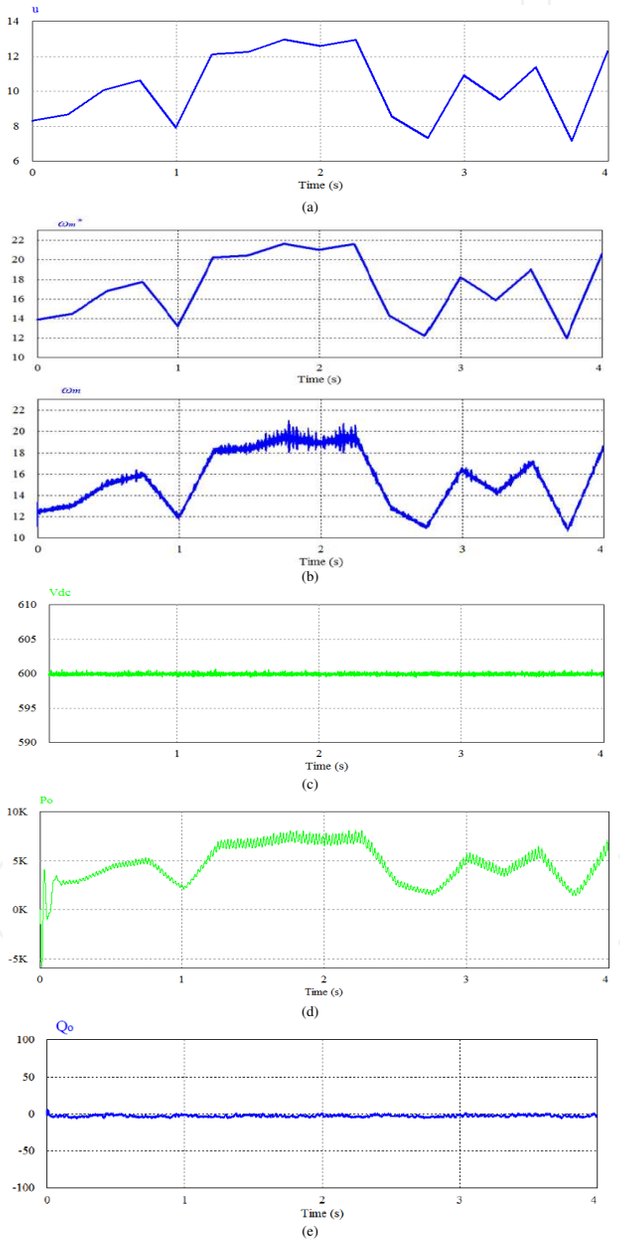

Figure 29. Different simulation waveforms: (a) Wind speed variation (7-13) m/s. (b) Actual and reference rotational speed (rad/s). (c) dc-link voltage (v). (d) Active power (watt). (e) Reactive power (Var).

5. Conclusions

Wind energy conversion system has high priority among the various renewable energy systems. Maximum power extraction from wind energy system became an important research topic due to the increase in output energy by using this technique. Wind speed sensorless MPPT control has been a very active area of research. In this study, a concise review of MPPT control methods has been presented for controlling WECS. On the other hand, there is a continuing effort to make converter and control schemes more efficient and cost effective in hopes of developing an economically viable solution of increasing environmental issues. Wind power generation has grown at a high rate in the past decade and will continue with power electronic technology advanced. The survey of MPPT algorithms have been classified into MPPT algorithms with wind speed sensor and MPPT algorithms without wind speed sensor. A co-simulation (PSIM/Simulink) program has been proposed for WECS where PSIM contains the power circuit of the WECS and Matlab/Simulink has the control circuit of the system. The WT is connected to the grid via back–to-back PWM-VSC. The generator side controller and the grid side controller have been done in Simulink. The main function of the generator side controller is to track the maximum power from wind through controlling the rotational speed of the turbine using fuzzy logic controller. The fuzzy logic algorithm for the maximum output power of the grid-connected wind power generation system using a PMSG has been proposed and implemented above. The PMSG was controlled in indirect-vector field oriented control method and its speed reference was determined using fuzzy logic controller. The grid-side converter controls the dc-link voltage at a desired value, 600V, for the proposed system. Active and reactive power control has been achieved by controlling q-axis and d-axis grid current components respectively. The d-axis grid current is controlled to be zero for unity power factor and the q-axis grid current is controlled to deliver the power flowing from the dc-link to the grid. The simulation results prove the superiority of FLC and the whole control system.

Appendix

Wind turbine		PMSG	
Nominal Output Power	19kw	R_s (stator resistance)	1m
Wind speed input	7:13 m/s (saw tooth)	L_d (d-axis inductance)	1m
Base Wind Speed	12 m/s	L_q (q-axis inductance)	1m
Base Rotational Speed	190 rpm	No. of Poles P	30
Moment of inertia	1m	Moment of inertia	100m
Blade pitch angle input	0º	Mech. Time Constant	1

Table 3. Parameters of wind turbine model and PMSG

Acknowledgements

The authors acknowledge the National Plan for sciences and Technology program (Project No.: ENE226-02-08) by King Saud University for the financial support to carry out the research work reported in this chapter.

Author details

Ali M. Eltamaly, A. I. Alolah and Hassan M. Farh

Department of Electrical Engineering, College of Engineering, King Saud University, Riyadh, Saudi Arabia

References

[1] Vahid, O, & Hassan, N. Maximum power extraction for a wind-turbine generator with no wind speed sensor. in Proc. on IEEE, Conversion and Delivery of Electrical Energy in the 21st Cen. (2008). , 1-6.

[2] Thomas, A, & Lennart, S. An overview of wind energy status (2002). Renewable and sustainable energy reviews 2002, 6:67-128.

[3] DuboisOptimized permanent magnet generator topologies for direct-drive wind turbines. Ph.D. dissertation, Delft Univ. Technol., Delft, The Netherlands; (2004).

[4] Anders, G. Design of direct-driven permanent-magnet generators for wind turbines. Ph.D. dissertation, Chalmers Univ. Technol., Goteborg, Sweden; (1996).

[5] Torbjörn, T, & Jan, L. Control by variable rotor speed of a fixed pitch wind turbine operating in a wide speed range. IEEE Trans. on Energy Conversion, EC-8, (1993). , 520-526.

[6] BuehringFreris. Control policies for wind energy Conversion System. Proc. Inst. Elect. Eng. C, (1981). , 128, 253-261.

[7] Erimis, H. B, Ertan, E, & Akpinar, F. Ulgut, Autonomous wind energy conversion systems with a simple controller for maximum power transfer, Proc. Inst. Elect. Eng. B, (1992). , 139, 421-428.

[8] ChedidMrad, Basma. Intelligent control of a class of wind energy conversion systems. IEEE Trans. on Energy Conversion, EC-14, (1999). , 1597-1604.

[9] Marcelo, S, Bimal, B, & Ronald, S. Fuzzy logic-based intelligent control of a variable speed cage machine wind generation system. IEEE Trans. on Power Electron., PE-12, (1997). , 87-94.

[10] EnslinWyk. A study of a wind power converter with micro-computer based maximum power control utilizing an over- synchronous electronic Scherbius cascade. Renewable Energy World (1993). , 2(6), 551-562.

[11] Quincy, W, & Liuchen, C. An intelligent maximum power extraction algorithm for inverter-based variable speed wind turbine systems. IEEE Transactions on Power Electronics (2004). , 19(5), 1242-1249.

[12] Quincy, W. Maximum wind energy extraction strategies using power electronic converters. PhD. dissertation, Univ. of New Brunswick, Canada, (2003).

[13] Hui, L, Shi, K. L, & Mclaren, P. G. Neural-network-based sensorless maximum wind energy capture with compensated power coefficient. IEEE Trans. Ind. Appl., (2005). , 41(6), 1548-1556.

[14] RajuFernandes, Chatterjee. A UPF power conditioner with maximum power point tracker for grid connected variable speed wind energy conversion system. Proc. of 1st Int. Conf. on PESA, Bombay, India, (2004). , 107-112.

[15] Majid, A. A, Yatim, A. H. M, & Chee, W. Tan. A Study of Maximum Power Point Tracking Algorithms for Wind Energy System. Proc. of 1st IEEE Conf. on Clean Energy and Technology CET, (2011). , 321-326.

[16] Mónica, C, Santiago, A, & Juan, C. B. Control of Permanent-Magnet Generators Applied to Variable-Speed Wind-Energy Systems Connected to the Grid. IEEE Trans. Energy Conversion, 21 March (2006). , 130-135.

[17] Seung-ho, S, Shin-il, K, & Nyeon-kun, H. Implementation and control of grid connected AC-DC-AC power converter for variable speed wind energy conversion system. IEEE, (2003). , 154-158.

[18] Ali, M. E. Modelling of wind turbine driving permanent Magnet Generator with maximum power point tracking system. J. King Saud Univ., Riyadh,(2007). , 19(2), 223-237.

[19] Mahmoud, M. H, Mohamed, O, Mahrous, E. A, & Mahmoud, A. S. Simple sensorless control technique of permanent magnet synchronous generator wind turbine. Proc. of IEEE Int. Conf. on Power and Energy,PEC201),Kuala Lumpur, Malaysia, (2010). , 512-517.

[20] Swagat, P, Mohanty, K. B, & Benudhar, S. Performance Comparison of a Robust Self Tuned Fuzzy Logic Controller used for Power Control in Wind Conversion Systems. Proc. of Modern Electric Power Systems, MEPS'10, Wroclaw, Poland, September (2010). , 20-22.

[21] Xingjia, Y, Changchun, G, Zuoxia, X, Yan, L, & Shu, L. Variable Speed Wind Turbine Maximum Power Extraction Based on Fuzzy Logic Control. Proc. of Int. Conf. on Intelligent Human-Machine Systems and Cybernetics, IEEE; (2009). , 202-205.

[22] Ahmed, G. A, Dong-choon, L, & Jul-ki, S. Variable speed wind power generation system based on fuzzy logic control for maximum power output tracking. in Proc. 35th Annual IEEE Power Electron. Specialists Conf., PESC, Aachen, Germany, (2004). , 3, 2039-2043.

[23] Tanaka, T, & Toumiya, T. Output control by hill-climbing method for a small scale wind power generating system. Renewable Energy, (1997). , 12(4), 387-400.

[24] Tan, K, & Islam, S. Optimum control strategies in energy conversion of PMSG wind turbine system without mechanical sensors. IEEE Trans., (2004). , EC-19, 392-399.

[25] Datta, R, & Ranganathan, V. T. A method of tracking the peak power points for a variable speed wind energy conversion system. IEEE Trans. on Energy Conversion, March (2003). , EC-18, 163-168.

[26] Brendan, F, Damian, F, Leslie, B, Nick, J, David, M, Mark, O, Richard, W, & Olimpo, A. Wind power integration: connection and system operational aspects. Proc. IET Power and Energy Series, (2007). , 50, 77-85.

[27] Siegfried, H. Grid Integration of Wind Energy Conversion Systems. John Wiley & Sons, Germany; (2006).

[28] Gary, L. J. Wind Energy Systems. Prentice Hall, Englewood cliffs; (2003).

[29] Peter, V. Sensorless Vector and Direct Torque Control. Oxford science publications,New York, (1998).

[30] Orlando, M, Liserre, V. G, & Monopoli, A. Dell'Aquila. Speed Sensorless Control of a PMSG for Small Wind Turbine Systems. Proc. of IEEE International Symposiumon Industrial Electronics, ISlE, Seoul, Korea, July (2009). , 5-8.